# Hyperasymptotics for integrals with saddles

By M. V. Berry and C. J. Howls

*H. H. Wills Physics Laboratory, Tyndall Avenue, Bristol BS8 1TL, U.K.*

Integrals involving $\exp\{-kf(z)\}$, where $|k|$ is a large parameter and the contour passes through a saddle of $f(z)$, are approximated by refining the method of steepest descent to include exponentially small contributions from the other saddles, through which the contour does not pass. These contributions are responsible for the divergence of the asymptotic expansion generated by the method of steepest descent. The refinement is achieved by means of an exact 'resurgence relation', expressing the original integral as its truncated saddle-point asymptotic expansion plus a remainder involving the integrals through certain 'adjacent' saddles, determined by a topological rule. Iteration of the resurgence relation, and choice of truncation near the least term of the original series, leads to a representation of the integral as a sum of contributions associated with 'multiple scattering paths' among the saddles. No resummation of divergent series is involved. Each path gives a 'hyperseries', depending on the terms in the asymptotic expansions for each saddle (these depend on the particular integral being studied and so are non-universal), and certain 'hyperterminant' functions defined by integrals (these are always the same and hence universal). Successive hyperseries get shorter, so the scheme naturally halts. For two saddles, the ultimate error is approximately $\epsilon^{2.386}$, where $\epsilon$ (proportional to $\exp(-A|k|)$ where $A$ is a positive constant), is the error in optimal truncation of the original series. As a numerical example, an integral with three saddles is computed hyperasymptotically.

## 1. Introduction

We intend to discuss very accurate asymptotics for a class of integrals commonly occurring in pure and applied mathematics and physics, namely

$$I^{(n)}(k) = \int_{C_n(\theta_k)} \mathrm{d}z\, g(z) \exp\{-kf(z)\}. \tag{1}$$

Here $|k|$ is the large asymptotic parameter, and it will be convenient to regard $k \equiv |k| \exp(\mathrm{i}\theta_k)$ as complex. The functions $f$ and $g$ are analytic in a region which we will specify later. There are several saddles (stationary points) of $f$, which we assume to be simple zeros of the derivative $f'(z)$. The infinite oriented contour $C_n(\theta_k)$ is the path of steepest descent through the $n$th saddle, at $z = z_n$, along the two valleys, issuing from $z_n$, of the real part of the exponential. It is common to encounter integrals where the contour – for example, the real axis – is not a path of steepest descent, but in such cases the contour can be deformed to give the function as a sum of integrals of the type (1).

Thus (1) defines a function of $k$ for each saddle $n$; if $f$ is an $M$th order polynomial, there are $M-1$ saddles. As is well known, the method of steepest descent (De Bruijn

*Proc. R. Soc. Lond.* A (1991) **434**, 657–675
*Printed in Great Britain*

1958), based on expanding the integrand about $z_n$, generates for each integral an asymptotic series in powers of $k^{-1}$, multiplying a leading exponential $\exp\{-kf_n\}$, where $f_n \equiv f(z_n)$. As well as yielding extremely useful approximations, the method is fundamental in physics (providing for example connections between wave and ray optics, quantum and classical mechanics, and statistical mechanics and thermodynamics). Nevertheless, the series diverges, and the common view is that it can represent the exact integral $I^{(n)}$ only within an accuracy comparable with the size of the least term.

Here we show how much greater accuracy, and deeper understanding, can be obtained with the aid of the *principle of resurgence*, inspired by the works of Dingle (1973) and Écalle (1981, 1984), which we express in the following way. The reason for the divergence of the asymptotic series for $I^{(n)}$ is the existence of *other saddles* $z_{m\neq n}$, through which $C_n$ does not pass. These contribute smaller exponentials, 'beyond all orders' of $k^{-1}$. Therefore the divergent part of the series must contain information about these other saddles. This is also true for the other asymptotic series, based on the other saddles $z_m$. Thus all the asymptotic series are related by a requirement of mutual consistency: each must contain, in its late terms, all the terms of the asymptotic series from all the other saddles. This information is present in coded form, because the series all diverge.

Its systematic decoding, to obtain successive approximations more accurate than the least term of the original series, is what in our recent paper (Berry & Howls 1990*a*, hereinafter called I) we called 'hyperasymptotics'. This terminology was introduced to distinguish the novel procedure from the following two familiar schemes. First, ordinary (Poincaré) asymptotics, namely stopping at a fixed order $N$ independent of $|k|$; as is well known, the error here is of order $|k|^{-(N+1)}$. Second, 'superasymptotics', namely stopping at the least term (a procedure originally used by Stokes (1847)); the order of this term is proportional to $|k|$, and the error is now of order $\exp(-A|k|)$ where $A$ is a positive constant. With hyperasymptotics we achieved an error $\exp(-2.386A|k|)$.

The functions we studied in I were solutions of second-order differential equations, of Schrödinger type, dominated by a single transition point. Such equations have two solutions, each represented in lowest-order WKB theory by an exponential. Hyperasymptotics was based on repeated Borel summation, based on a formal resurgence relation, discovered by Dingle (1973), relating the late terms of the series multiplying one exponential and the early terms of the series multiplying the other. That example was special because it involved only two exponentials and the terms in the two asymptotic series were the same, up to signs.

Hyperasymptotics based on the integral (1) is much more general because many exponentials are involved and the terms in all the associated asymptotic series are different. The treatment differs from that in I, in that it does not involve the resummation of divergent series. Instead, we shall employ the iteration of an exact and finite (i.e. not formal) resurgence formula, giving the remainder of the truncated asymptotic expansion for $I^{(n)}$ in terms of the integrals $I^{(m)}$ through certain other saddles, selected by a rule depending on the topology of $f(z)$. This integral resurgence formula generalizes the Stieltjes-transform relation postulated in recent work by Boyd (1990).

## 2. Steepest-descent expansion

The steepest path through $z_n$, that is $C_n(\theta_k)$, is defined by $k(f(z)-f_n)$ real and increasing away from $z_n$. As the phase $\theta_k$ is altered, the steepest path near $z_n$ rotates half as fast, so that when $k$ returns to its original value, after a phase change of $2\pi$, the orientation of $C_n(\theta_k)$ has reversed, and $I^{(n)}(k)$ has changed sign. Therefore the integrals $I^{(n)}(k)$ are double-valued, and the functions $T^{(n)}(k)$, defined by

$$I^{(n)}(k) \equiv k^{-\frac{1}{2}} \exp\left[-kf_n\right] T^{(n)}(k),$$

i.e.

$$T^{(n)}(k) = k^{\frac{1}{2}} \int_{C_n(\theta_k)} \mathrm{d}z\, g(z) \exp\left\{-k[f(z)-f_n]\right\} \tag{2}$$

are single valued.

These functions are not, however, continuous, because the steepest paths jump whenever they pass through one of the other saddles $m \neq n$. One way to see that jumps must occur is to consider the case where $f(z)$ is an $M$th-order polynomial, so that there are $M-1$ saddles. Then $f(z)$ grows at infinity like $z^M$, so that, when $\theta_k$ changes, $C_n(\theta_k)$ rotates at infinity $\frac{1}{2}M$ times as fast as near $z_n$; therefore when $M > 2$ (that is, when there is more than one saddle) the steepest paths must jump if they are merely to reverse orientation during a circuit of $k$ in its plane. Each jump is an example of the Stokes phenomenon, which as we will explain later is in this formalism a discontinuity, rather than a smooth transition (Berry 1989*a*), because we have *chosen* the path to be the one of steepest descent.

We require the coefficients $T_r^{(n)}$ in the formal asymptotic expansion

$$T^{(n)}(k) = \sum_{r=0}^{\infty} \frac{T_r^{(n)}}{k^r}. \tag{3}$$

The expansion is formal because, as is well known and as we shall study in detail later in this section, it diverges.

To obtain the coefficients, and also to develop our resurgence formula, we shall use a representation of $T^{(n)}(k)$ as a double integral. This is based on the transformation to the new integration variable

$$u(z) \equiv k[f(z)-f_n]. \tag{4}$$

For each value of $z$ on $C_n(\theta_k)$, $u$ is real and non-negative. For each value of $u$ (except $u = 0$), there are two values of $z$ (figure 1): $z_+(u)$, on the half of the steepest descent path emerging from $z_n$, and $z_-(u)$, on the half leading into $z_n$. The transformation gives

$$T^{(n)}(k) = \int_0^{\infty} \mathrm{d}u \frac{\exp(-u)}{k^{\frac{1}{2}}} \left\{ \frac{g(z_+(u))}{f'(z_+(u))} - \frac{g(z_-(u))}{f'(z_-(u))} \right\}. \tag{5}$$

The quantity in curly brackets can be written as the contour integral

$$\left\{ \frac{g(z_+(u))}{f'(z_+(u))} - \frac{g(z_-(u))}{f'(z_-(u))} \right\} = \frac{1}{2\pi \mathrm{i} u^{\frac{1}{2}}} \oint_{\Gamma_n(\theta_k)} \mathrm{d}z \frac{g(z)[k\{f(z)-f_n\}]^{\frac{1}{2}}}{f(z)-f_n-u/k}, \tag{6}$$

where $\Gamma_n(\theta_k)$ is the positive (anticlockwise) loop surrounding $C_n(\theta_k)$ (figure 2). The square root, defined as having phase zero on the path $C_n(0)$ emerging from the saddle, and $\pi$ on the path leading into it, is single-valued on $C_n(\theta_k)$ because of the double-

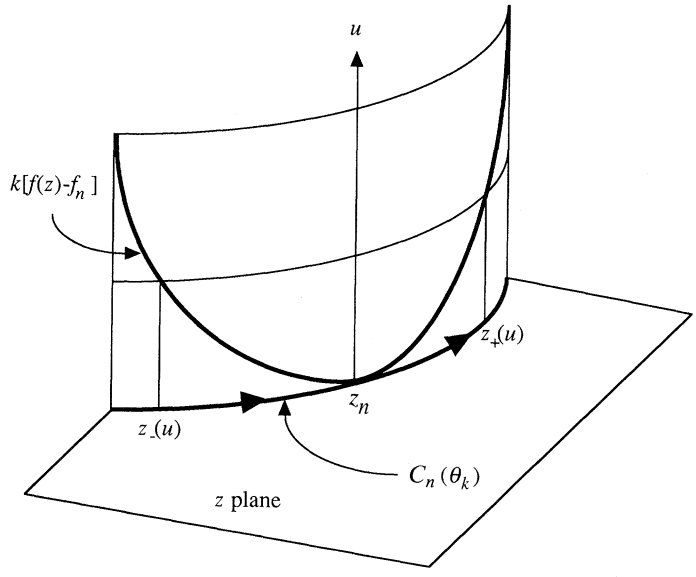


Figure 1. Double-valued mapping (equation (4)) from $z$ to $u$.

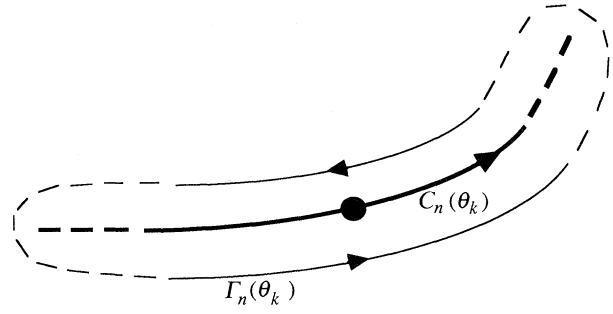


Figure 2. Steepest path $C_n(\theta_k)$ through saddle $n$, and loop $\Gamma_n(\theta_k)$ enclosing it.

valuedness of (4). Equations (6) and (5) now give the desired representation, which will form the basis of all that follows:

$$T^{(n)}(k) = \frac{1}{2\pi \mathrm{i}} \int_0^\infty \mathrm{d}u \frac{\exp(-u)}{u^{\frac{1}{2}}} \oint_{\Gamma_n(\theta_k)} \mathrm{d}z \frac{g(z)[f(z)-f_n]^{\frac{1}{2}}}{f(z)-f_n-u/k}. \tag{7}$$

Expanding the denominator in powers of $k^{-1}$ gives the coefficients in (3) as (cf. Dingle 1973, p. 119)

$$T_r^{(n)} = \frac{(r-\frac{1}{2})!}{2\pi \mathrm{i}} \oint_n \mathrm{d}z \frac{g(z)}{[f(z)-f_n]^{r+\frac{1}{2}}}, \tag{8}$$

where the subscript $n$ indicates that now the contour $\Gamma_n(\theta_k)$ has been shrunk to a small positive loop around $z_n$. These integrals can be evaluated exactly in terms of the coefficients in the expansions of $f$ and $g$ about $z_n$, to yield the explicit (and complicated) expressions (Dingle 1973, p. 119ff) for the terms in the saddle-point expansion. For example, the leading term $r = 0$ is

$$T_0^{(n)} = (2\pi/f_n'')^{\frac{1}{2}} g_n \tag{9}$$

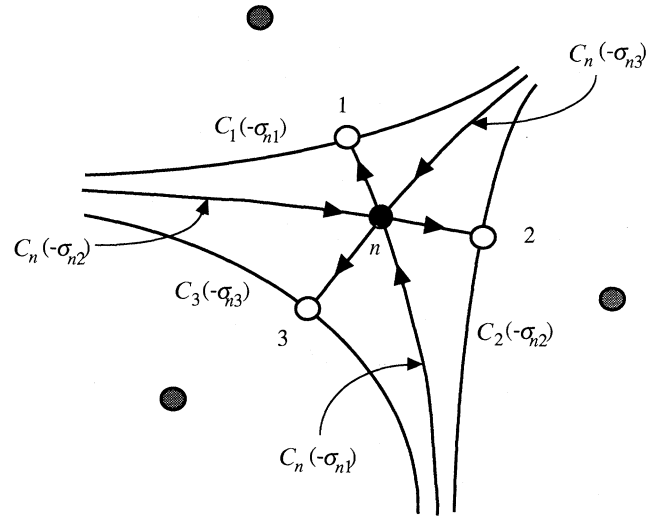


Figure 3. Special phase contours of $f(z)-f_n$ (steepest paths) through saddle $n$ (●), encountering adjacent saddles $m = 1, 2, 3$ (○), with their steepest paths; non-adjacent saddles (shaded circles) are also shown.

(here, as before, primes denote derivatives and subscripts $n$ denote quantities evaluated at $z_n$).

## 3. Resurgence relation

We expand the denominator in (7) to isolate the first $N$ terms, using

$$\frac{1}{1-x} = \sum_{r=0}^{N-1} x^r + \frac{x^N}{1-x}. \tag{10}$$

Thus

$$T^{(n)}(k) = \sum_{r=0}^{N-1} \frac{T_r^{(n)}}{k^r} + R^{(n)}(k,N), \tag{11}$$

where $T_r^{(n)}$ are the coefficients (8) and the remainder $R^{(n)}$ is

$$R^{(n)}(k,N) = \frac{1}{2\pi \mathrm{i} k^N} \int_0^\infty \mathrm{d}u \exp(-u) u^{N-\frac{1}{2}} \times \oint_{\Gamma_n(\theta_k)} \mathrm{d}x \frac{g(z)}{[f(z)-f_n]^{N+\frac{1}{2}}\{1-u/k(f(z)-f_n)\}}. \tag{12}$$

Next we deform the contour $\Gamma_n(\theta_k)$ in a particular way, which as will now be explained depends on the topology of $f(z)$. Consider all the steepest paths through the saddle $n$, for different $\theta_k$. As illustrated in figure 3, some of them are special in that they encounter other saddles $m$. We call these the saddles *adjacent* to $n$. From now on we will make extensive use of this concept of adjacency.

To specify the paths through the adjacent saddles we define the 'singulants' (a term introduced by Dingle (1973))

$$F_{nm} \equiv |F_{nm}| \exp(\mathrm{i}\sigma_{nm}) \equiv f_m - f_n. \tag{13}$$

The special steepest paths are those corresponding to $kF_{nm}$ positive real, that is

$$k = |k| \exp(-\mathrm{i}\sigma_{nm}), \quad \text{i.e. } \theta_k = -\sigma_{nm}. \tag{14}$$

The steepest path $C_n(-\sigma_{nm})$ turns sharply through a right angle at $z_m$, to continue descending into a valley of $\exp\{-k[f(z)-f_n]\}$ (whether the path turns right or left depends on whether $\theta_k$ approaches $-\sigma_{nm}$ from below or above; cf. figure 4 later).

We deform $\Gamma_n(\theta_k)$ by expanding it onto the union of arcs at infinity and arcs through the adjacent saddles $m$. These arcs are the steepest paths through $m$ with $k$ given by (14), that is $C_m(-\sigma_{nm})$. We obtain, symbolically, for (12),

$$\oint_{\Gamma_n(\theta_k)} \mathrm{d}z \ldots = \sum_m (-1)^{\gamma_{nm}} \int_{C_m(-\sigma_{nm})} \mathrm{d}z \ldots, \tag{15}$$

where the sum is over the adjacent saddles and $\gamma_{nm}$ is an 'orientation anomaly', 0 if the arc of the expanded $\Gamma_n(\theta_k)$ has the same orientation as $C_m(-\sigma_{nm})$, and 1 otherwise. For the relation (15) to hold, three conditions must be satisfied. First, $|g|/|f|^{N+\frac{1}{2}}$ must decay at infinity faster than $1/|z|$, in order for the infinite arcs to give zero contribution. Second, there must be no zeros of the quantity in braces in the denominator of (12), for any $u$, in the region of the $z$ plane swept by this contour expansion; in Appendix A we study these 'dangerous zeros' (which for $u = 0$ are also branch points of the integrand), and show that they do lie outside this region. Third, the functions $f$ and $g$ must contain no singularities in this same region; this is the analyticity condition mentioned in §1.

Next, along the arc of the expanded path which passes through $m$ we transform the $u$ integration variable in (12) to $v$, according to the relation

$$u \equiv v[f(z)-f_n]/F_{nm} = v + v[f(z)-f_m]/F_{nm}. \tag{16}$$

Like $u$, $v$ is real and positive. The remainder (12) becomes

$$R^{(n)}(k,N) = \frac{1}{2\pi\mathrm{i}k^N} \sum_m \frac{(-1)^{\gamma_{nm}}}{F_{nm}^{N+\frac{1}{2}}} \int_0^\infty \mathrm{d}v \frac{\exp(-v)}{1-v/(kF_{nm})} v^{N-\frac{1}{2}} \times \int_{C_m(-\sigma_{nm})} \mathrm{d}z\, g(z) \exp\{-v[f(z)-f_m]/F_{nm}\}. \tag{17}$$

The $z$ integral is of the form (1), and so, using (2), we see that the remainder has been expressed as a sum over integrals through the adjacent saddles:

$$R^{(n)}(k,N) = \frac{1}{2\pi\mathrm{i}} \sum_m \frac{(-1)^{\gamma_{nm}}}{(kF_{nm})^N} \int_0^\infty \mathrm{d}v \frac{v^{N-1}\exp(-v)}{1-v/(kF_{nm})} T^{(m)}\left(\frac{v}{F_{nm}}\right). \tag{18}$$

Combining this with (11), we obtain the following exact resurgence formula, which will be the basis for hyperasymptotics:

$$T^{(n)}(k) = \sum_{r=0}^{N-1} \frac{T_r^{(n)}}{k^r} + \frac{1}{2\pi\mathrm{i}} \sum_m \frac{(-1)^{\gamma_{nm}}}{(kF_{nm})^N} \int_0^\infty \mathrm{d}v \frac{v^{N-1}\exp(-v)}{1-v/(kF_{nm})} T^{(m)}\left(\frac{v}{F_{nm}}\right). \tag{19}$$

This formula provides an explicit and exact form for the remainder in the method of steepest descent. When we use it for hyperasymptotics we shall choose $N$ to be the order of the least term of the asymptotic series (3). But it holds for any $N$, and by choosing $N$ fixed and letting $|k| \to \infty$ we can use it to establish at once that (3) is an asymptotic series in the sense of Poincaré, that is the remainder is of order $|k|^{-N}$ (for a development of this idea, see Boyd (1991)).

An immediate application of (19) is to the derivation of formal resurgence relations for the coefficients $T_r^{(n)}$ in the expansion about the $n$th saddle. Choosing $N=0$ (so that the sum over $r$ is empty), substituting the series (3) for the saddles $n$ and $m$ into both sides of (19), and identifying coefficients of powers of $k^{-1}$, we obtain

$$\begin{aligned} T_r^{(n)} &= \frac{1}{2\pi \mathrm{i}} \sum_m (-1)^{\gamma_{nm}} \sum_{t=0}^{\infty} \frac{(r-t-1)!}{F_{nm}^{r-t}} T_t^{(m)} \\ &= \frac{1}{2\pi \mathrm{i}} \sum_m (-1)^{\gamma_{nm}} \frac{(r-1)!}{F_{nm}^r} \left[ T_0^{(m)} + \frac{F_{nm}}{r-1} T_1^{(m)} \dots \right]. \end{aligned} \tag{20}$$

This gives the late terms ($r \gg 1$) of the series for a given saddle as a sum over the early terms of the series for the adjacent saddles. The leading contribution, from the adjacent saddle $m^*$ with the smallest singulant $|F_{nm}|$, is

$$T_r^{(n)} \approx T_0^{(m^*)} \frac{(-1)^{\gamma_{nm^*}} (r-1)!}{F_{nm^*}^r} \tag{21}$$

and has the familiar 'factorial/power' form. (In the interesting special case where two or more adjacent saddles have the same |singulant|, their contributions add.) The complete resurgence relation (20) is formal because the factorials are infinite when $t > r-1$, but it does give an asymptotic expansion for the late terms. By Borel summation, the formal relation can be converted into an exact one, but this is just (19) (indeed we originally obtained (19) in this way, after conjecturing (20)).

In the special case of two saddles (for which there is just one adjacent saddle $m$) the resurgence relation (20) was discovered by Dingle (1973) not only for integrals (where it was rediscovered by Balian *et al.* 1979) but also for the analogous case of second-order differential equations (where it was rediscovered by Rakovic & Solov'ev (1989)).

Now we show how the resurgence formula (19) incorporates the Stokes phenomenon (Stokes 1864). This is the appearance of a subdominant exponential (Berry 1989*b*) as the contour $C_n(\theta_k)$ sweeps through one of the adjacent saddles $m$. As we have seen, one way to make this happen is to vary $\theta_k$ through $-\sigma_{nm}$, defined by (13). Let

$$k = |k| \exp\{\mathrm{i}(-\sigma_{nm} + \delta)\} \tag{22}$$

and let $\delta$ sweep through zero. The behaviour of the integration contour $C_n(\theta_k)$ during this process is illustrated in figure 4, and shows that $T^{(n)}$ has a discontinuity, whose magnitude must be

$$\begin{aligned} T^{(n)}(|k| \exp\{\mathrm{i}(-\sigma_{nm} + 0_+)\}) - T^{(n)}(|k| \exp\{\mathrm{i}(-\sigma_{nm} + 0_-)\}) \\ = (-1)^{\gamma_{nm}+1} \exp(-kF_{nm})\, T^{(m)}(|k| \exp\{-\mathrm{i}\sigma_{nm}\}) \end{aligned} \tag{23}$$

(the extra minus sign can be confirmed by diagrams corresponding to the two possible orientation anomalies). This jump is exponentially small because $kF_{nm}$ is positive real. Exactly the same jump is given by (19); its origin is the pole at $v = kF_{nm}$, which sweeps up through the integration contour (positive real axis) as $\delta$ increases through zero (the extra minus comes from the sign of the denominator in (19)). Note that the discontinuity is independent of the truncation order $N$, a known aspect of the Stokes phenomenon (Dingle 1973).

At first sight, the discontinuity might appear inconsistent with the universal smooth behaviour across Stokes lines, established by Berry (1989*a*). However, the discordance arises from a difference of definition. In this paper it has been convenient

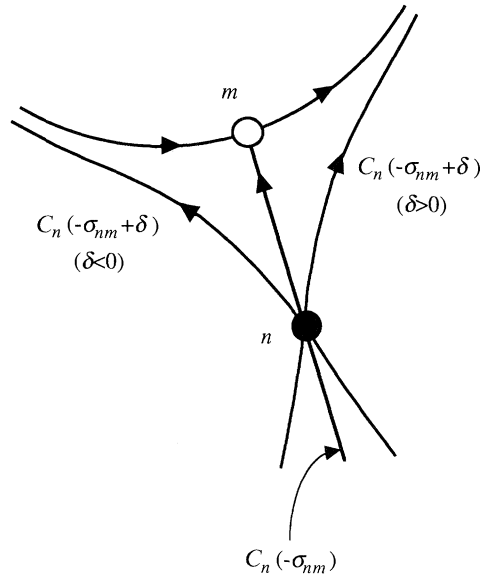


Figure 4. Jump in the steepest path through $n$ as adjacent saddle $m$ is passed, corresponding to the appearance of a subdominant exponential (Stokes's phenomenon).

to define the integration contour in (1) as the single infinite arc through $z_n$, connecting valleys of the integrand. This contour is $k$-dependent, and jumps when $\theta_k$ passes $-\sigma_{nm}$. On the other hand, it is more usual to define integrals with contours between infinite limits independent of $k$, which are therefore analytic functions of $k$ near $\theta_k = -\sigma_{nm}$. The conventional definition can easily be incorporated in the present framework by allowing the pole in (19) to drag the integration contour with it when it passes the positive real axis, as we have explained in detail in §5 of I.

## 4. Hyperasymptotic multiple scattering

The iteration of the resurgence formula (19) is more complicated than in I, because now there can be several adjacent saddles (as embodied in the sum over $m$ in (19)), rather than just two. After iterating (19) $s$ times, we obtain

$$T^{(0)} = \sum_{r=0}^{N_0-1} T_r^{(0)} K_r^{(0)} + \sum_{1} \sum_{r=0}^{N_1-1} T_r^{(1)} K_r^{(01)} + \sum_{1}\sum_{2} \sum_{r=0}^{N_2-1} T_r^{(2)} K_r^{(012)} + \ldots \sum_{1} \ldots \sum_{s} \left( \sum_{r=0}^{N_s-1} T_r^{(s)} K_r^{(01\ldots s)} + R^{(01\ldots s)} \right). \quad (24)$$

To avoid long formulae we have here used an abbreviated notation: 0 stands for the starting saddle $n_0$, 1 for the saddles $n_1$, adjacent to $n_0$, reached in the first iteration, ... $s$ for the saddles $n_s$ reached in the $s$th iteration. For reasons to be explained later, we allow the arbitrary truncation orders $N$ to change at each iteration. As well as the coefficients $T_r^{(s)}$ in all the primitive asymptotic series (3), this formula involves 'hyperterminant' integrals $K_r^{(01\ldots s)}$ generalizing those in I, and the remainders $R^{(01\ldots s)}$.

The hyperterminants and the remainders depend on

$$y_{p-1,\,p,\,p+1} \equiv F_{p-1,\,p}/F_{p,\,p+1}. \quad (25)$$

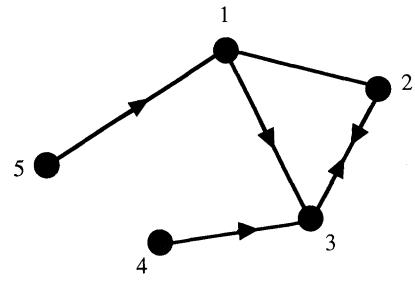


Figure 5. A possible adjacency diagram for five saddles, with arrows pointing to the nearest; thus adjacent to 1 are 2, 3 and 5, with 3 nearest.

The hyperterminants are

$$K_r^{(0)} = 1/k^r$$

$$K_r^{(01\ldots s)} = \left(\prod_{p=0}^{s-1} \int_0^\infty \mathrm{d}v_p\right) J_r^{(01\ldots s)}, \tag{26}$$

where

$$J_r^{(01)} = \frac{(-1)^{\gamma_{01}}}{2\pi \mathrm{i} k^{N_0} F_{01}^{N_0 - r}} \frac{v_0^{N_0 - r - 1} \exp(-v_0)}{(1 - v_0/kF_{01})}, \tag{27}$$

$$J_r^{(01\ldots s)} = \frac{(-1)^{\gamma_{s-1,s}}}{2\pi \mathrm{i} F_{s-1,s}^{N_{s-1} - r}} \frac{v_{s-1}^{N_{s-1} - r - 1} \exp(-v_{s-1})}{(1 - (v_{s-1}/v_{s-2}) y_{s-2,s-1,s})} J_{N_{s-1}}^{(01\ldots s-1)} \quad (s \geqslant 2).$$

The remainder after $s$ iterations is

$$R^{(0\ldots s)} = \left(\prod_{p=0}^{s} \int_0^\infty \mathrm{d}v_p\right) \sum_{s+1} J_0^{(0\ldots s+1)} T^{(s+1)}\left(\frac{v_s}{F_{s,s+1}}\right). \tag{28}$$

The scheme (24)–(28) gives an exact representation of the integral (1). It looks complicated, and might appear to give no advantage over the original representation as a single integral, because the hyperterminants are multiple integrals whose order increases with order of iteration. However, the hyperterminants are *universal functions* of the singulants and truncations, which need be evaluated only once; the non-universal aspects of the scheme, distinguishing the particular integral being evaluated, are embodied in the coefficients $T_r^{(s)}$ in (24).

It is convenient to interpret (24) by regarding iteration as multiple scattering between successive groups of adjacent saddles. The first term (involving $K^{(0)}$) corresponds to no scatterings and involves the single saddle 0, the second term (involving $K^{(01)}$) corresponds to single scatterings from 0 to one of the adjacent saddles 1, etc. A diagrammatic representation is appropriate. The first step is to construct an 'adjacency diagram' (figure 5) in which the saddles are depicted as points in a plane (e.g. the original $z$ plane), and each is connected to those adjacent to it (the significance of the arrows will be explained later). A multiple scattering path is now defined as a sequence of saddles, each adjacent to the next. The set of multiple scattering paths can be constructed as illustrated in figure 6. The number of paths proliferates rapidly: in figure 6, which corresponds to five saddles, connected as in figure 5, the first three iterations generate 15 paths. When there are just two saddles (the case considered in I) there is only one scattering path, bouncing back and forth between them. For such backscattering, the definitions (13) and (25) give $y = -1$, so that the denominators in the integrals (26) and (27) do not vanish. In general, a denominator will vanish if the corresponding $y$ is positive real, but we

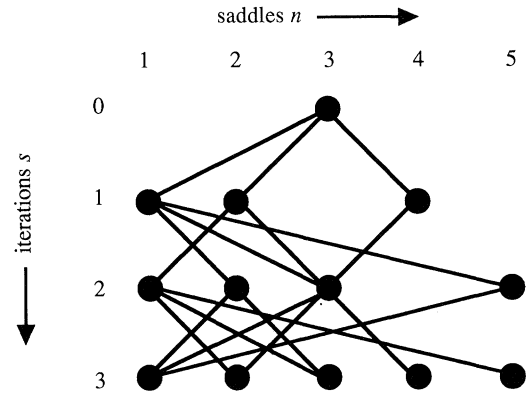


Figure 6. The fifteen multiple scattering paths from saddle 3, generated by the adjacency diagram of figure 5 by hyperasymptotic iteration.

ignore this exceptional case (which is the signature of a 'double Stokes phenomenon', in which a steepest path from one saddle hits a second, turns through a right angle and then encounters a third).

In (24) each scattering path contributes a 'hyperseries' over the orders $r$ of the original asymptotic expansion, whose limits are $r = 0$ and $r = N_s - 1$ (for a path with $s$ scatterings). Unless the truncations $N_s$ are specified, the scheme is not unique. In any truncation scheme, each hyperseries must be shorter than its predecessor, because from (27) the hyperterminant integrals (26) do not converge unless $N_{p+1} < N_p$. This has two consequences. First, the sequence of hyperseries along each scattering path must eventually halt – when it generates a hyperseries containing a single term. Second, each sequence contains only a finite amount of information, because it involves only a finite number of primitive coefficients $T_r^{(n)}$ (the number being the truncation $N$ when the saddle $n$ first appears).

Because of this finite information, hyperasymptotics will halt with a finite remainder. It might seem natural to make the remainder as small as possible by choosing a large starting truncation, and indeed arbitrary accuracy can be obtained in this way, as we showed in I. However, such schemes are unnatural because they lead to series whose terms get very large before decreasing, thereby violating the 'live now, pay later' philosophy underlying asymptotics, where ultimate accuracy is sacrificed for improvement at every stage. (Without this philosophy, one could as well use the *convergent* series in $k$ which can be found in many cases, but which are computationally inefficient when $|k|$ is large.)

To preserve the spirit of asymptotics, we shall consider each scattering path separately and demand that the successive series it generates are optimally truncated; that is, truncated near their least terms, so that the remainders $R^{(0\cdots s)}$ for each $s$ along the path are smallest. In determining the optimal $N$s, we shall make use of the concept of the *nearest* saddle to a given saddle $n$, defined as the adjacent saddle $m$ with the smallest singulant modulus $|F_{nm}|$. As in (21), we shall denote nearest saddles by asterisks, so that, for example, the path 0123* is the path starting at saddle 0, going through given saddles 1 and 2, and ending at the saddle 3* nearest to 2. In an adjacency diagram such as figure 5, nearest saddles can be indicated by arrows.

To determine the optimal truncations we must estimate the remainders $R^{(0\cdots s)}$.

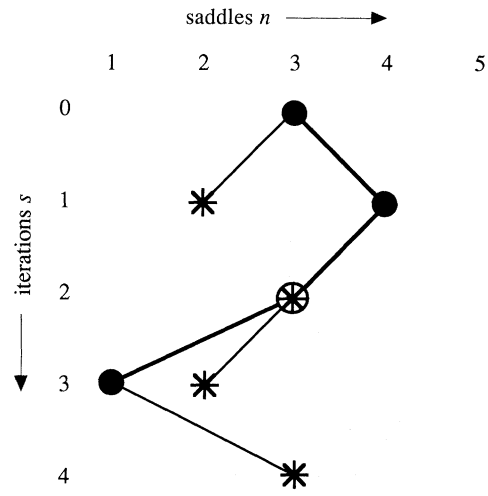


Figure 7. One of the multiple scattering paths in figure 6 (thick line) together with nearest saddles (*) contributing at each level of truncation (shown linked to their progenitors by thin lines). For the second iteration the nearest saddle (3) is also the next saddle on the actual path.

This we do by approximating $T^{(s+1)}$ to lowest order with (21) (thereby replacing the sum over the $(s+1)$th order saddles, adjacent to the $s$th, by the saddle $(s+1)^*$ nearest to the $s$th). Moreover, the denominators in (27) are of order unity (this follows from the procedure, used in I, of replacing the $v$s in the denominators by the maxima of the rest of the integrands), and so we approximate them by unity. The $v$s are now uncoupled, and the remainders can be evaluated as products of factorials. These can be simplified with the aid of Stirling's approximation, and we obtain

$$\left.\begin{aligned} |R^{(0)}| &\approx \frac{N_0^{N_0-\frac{1}{2}}\exp(-N_0)}{\sqrt{(2\pi)}\,|kF_{01^*}|^{N_0}}|T_0^{(1^*)}|, \\ |R^{(0\ldots s)}| &\approx \frac{N_s^{N_s-\frac{1}{2}}\exp(-N_0)}{(2\pi)^{(s+1)/2}\,|k|^{N_0}\,|F_{s,(s+1)^*}|^{N_s}}\prod_{p=0}^{s-1}\frac{(N_p-N_{p+1})^{(N_p-N_{p+1}-\frac{1}{2})}}{|F_{p,p+1}|^{N_p-N_{p+1}}}|T_0^{((s+1)^*)}| \end{aligned}\right\} \tag{29}$$

Successive minimization along the scattering path now gives

$$\left.\begin{aligned} N_0 &= \mathrm{Int}\,|kF_{01^*}|, \\ N_s &= \mathrm{Int}\frac{N_{s-1}}{1+|y_{s-1,s,(s+1)^*}|} = \mathrm{Int}\frac{N_{s-1}}{1+|F_{s-1,s}/F_{s,(s+1)^*}|}. \end{aligned}\right\} \tag{30}$$

Henceforth we shall omit the 'Int' symbols. The nearest saddle to $s$, that is $(s+1)^*$, cannot be more distant than the preceding saddle $s-1$, so that

$$|y_{s-1,s,(s+1)^*}| \geqslant 1, \quad \text{and} \quad N_s \leqslant \tfrac{1}{2}N_{s-1}. \tag{31}$$

Thus each hyperseries is at most half the length of its predecessor. Figure 7 shows one of the scattering paths of figure 6, together with the nearest saddles which contribute to the successive truncations.

With these truncations, the optimal hyperasymptotic remainders can be estimated from (29). The zero-stage (superasymptotic) remainder is

$$|R^{(0)}| \approx \frac{\exp(-|kF_{01^*}|)}{\sqrt{(2\pi\,|kF_{01^*}|)}}|T_0^{(1^*)}|. \tag{32}$$

The improvement from the $(s-1)$th to the $s$th stage is

$$\left|\frac{R^{(0\ldots s)}}{R^{(0\ldots s-1)}}\right| \approx \frac{1+|y_{s-1,s,(s+1)^*}|}{\sqrt{(2\pi N_{s-1}|y_{s-1,s,(s+1)^*}|)}} \times \exp\left\{-N_{s-1}\ln\left[\frac{|F_{s,(s+1)^*}|+|F_{s-1,s}|}{|F_{s-1,s^*}|}\right]\right\}\left|\frac{T_0^{((s+1)^*)}}{T_0^{(s^*)}}\right|. \quad (33)$$

This does represent an improvement, rather than a degradation, because (31) and the definition of nearness guarantee that the argument of the logarithm exceeds unity, so that the exponent is positive. On average the improvements diminish, because the truncation limits decrease (equation 30). The improvement is greater if $s$ is a saddle far from $s-1$ (rather than the nearest saddle $s^*$), and less if the saddle $(s+1)^*$ nearest to $s$ is closer to $s$ than $s-1$ was.

In the special case of two saddles, equivalent to that considered in I, the formulae simplify considerably. There is only one adjacent saddle, and it is of course the nearest, so that (cf. (25)) $y_{s-1,s,s+1}=-1$ and (cf. (30)) the $s$th truncation limit is $N_s=|kF_{01}|/2^s$. The hyperasymptotic improvement (33) is

$$\left|\frac{R^{(0\ldots s)}}{R^{(0\ldots s-1)}}\right| \approx \frac{2^{s/2}}{\sqrt{(\pi|kF_{01}|)}}\exp\left\{-\frac{|kF_{01}|}{2^{s-1}}\ln 2\right\}. \quad (34)$$

It is the accumulation of these improvements which, together with (32), gives the final remainder $\exp\{-|kF_{01}|(1+2\ln 2)\}=\exp\{-2.386|kF_{01}|\}$ obtained in I.

The optimal truncations (30), and the estimate (33) for the improvements in the remainder, hold for a given multiple scattering path. Each path can be followed to its end (when hyperasymptotics halts) and the final remainder estimated. In general the remainders will all be different. Obviously the overall accuracy of the scheme is controlled by the path with the largest final remainder. Therefore it is pointless to evaluate hyperseries along the other paths more precisely than this, so that hyperasymptotics for these other paths should be prematurely terminated at this level.

## 5. Example: Pearcey's integral

We shall calculate

$$\mathrm{P}(x,y)\equiv\int_C \mathrm{d}z\,\exp\{\mathrm{i}(\tfrac{1}{4}z^4+\tfrac{1}{2}xz^2+yz)\}, \quad (35)$$

where $C$ descends into the valleys at $\infty\exp(\mathrm{i}\pi/8)$ and $\infty\exp(5\mathrm{i}\pi/8)$. This integral was first studied (for real $x$ and $y$) by Pearcey (1946). Provided the contour passes through just one of the three saddles, this has the form (1), with $k=1$ (any other $k$ can be reduced to 1 by scaling $x$ and $y$), $g=1$ and

$$f(z;x,y)=-\mathrm{i}(\tfrac{1}{4}z^4+\tfrac{1}{2}xz^2+yz). \quad (36)$$

We choose the complex values

$$x=7,\quad y=1+\mathrm{i} \quad (37)$$

thereby ensuring that the magnitudes of the singulants are all different.

The positions of the saddles (where $z^3+xz+y=0$) are

$$\left.\begin{aligned} z_1&=+0.077\,621\,247\,095\,613-\mathrm{i}2.574\,820\,095\,698\,692,\\ z_2&=-0.143\,675\,227\,409\,104-\mathrm{i}0.142\,009\,934\,077\,984,\\ z_3&=+0.066\,053\,980\,313\,492+\mathrm{i}2.716\,830\,029\,776\,676,\end{aligned}\right\} \quad (38)$$

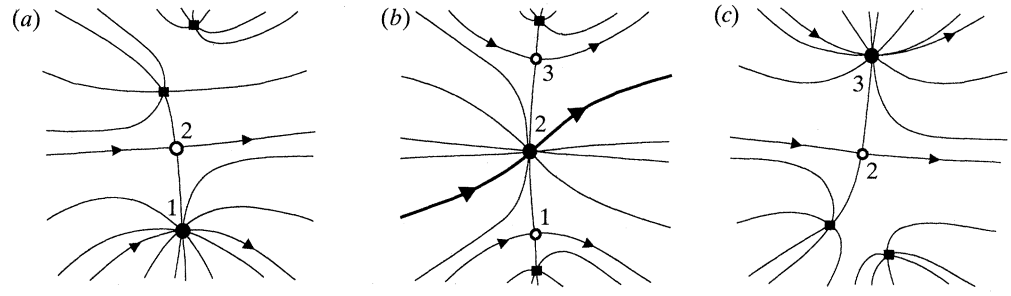


Figure 8. Some phase contours of $f(z)-f_n$, for the Pearcey integral (35)–(37) with (*a*) $n=1$, (*b*) $n=2$, (*c*) $n=3$. These saddles are denoted by ●, and adjacent saddles by ○; the bold line contour in (*b*) corresponds to the steepest path deformation of the contour in (35); dangerous zeros (Appendix A) are denoted (for $u=0$) by ■.

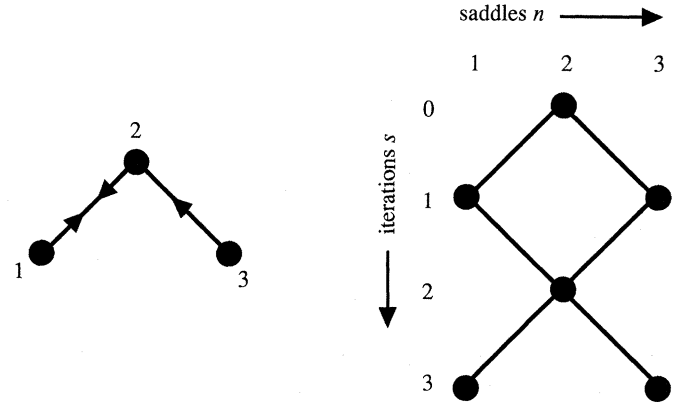


Figure 9. Adjacency diagram, and multiple scattering paths from saddle 2, corresponding to figure 8.

and the contour along the real axis can be deformed into the steepest path through saddle 2. Figure 8 defines the orientations of the contours through the three saddles, and shows the constant-phase lines (cf. figure 3) for the three functions $f(z)-f_n$. Thus 2 is adjacent to 1 and 3, and 1 and 3 are not adjacent. The adjacency diagram, and the multiple scattering paths from 2, are rather simple, as shown in figure 9. The orientation anomalies (cf. equation (15)) are

$$\gamma_{12}=1, \quad \gamma_{21}=0, \quad \gamma_{32}=0, \quad \gamma_{23}=1. \tag{39}$$

The three singulants are

$$\left.\begin{aligned} F_{12}(=-F_{21}) &= +2.429\,559\,462\,904\,937-\mathrm{i}\,9.601\,681\,152\,318\,827,\\ |F_{12}| &= 9.904\,294\,025\,047\,193,\\ F_{32} &= -2.858\,116\,325\,734\,320-\mathrm{i}\,14.897\,069\,623\,055\,830,\\ |F_{32}| &= 15.168\,767\,658\,765\,224,\\ F_{13} &= +5.287\,675\,788\,639\,256+\mathrm{i}\,5.295\,388\,470\,737\,003,\\ |F_{13}| &= 7.483\,358\,490\,796\,506. \end{aligned}\right\} \tag{40}$$

Therefore 1 is the nearer of the saddles adjacent to 2. We shall soon give the reason for including $F_{13}$ even though this singulant cannot contribute to hyperasymptotics because 1 and 3 are not adjacent.

The raw data of the hyperasymptotic scheme (24) are the asymptotic coefficients $T_r^{(n)}$ appearing in (3). From the contour integral (8) we obtain (by expanding the denominator binomially)

$$T_r^{(n)} = \frac{-2^{3r+\frac{1}{2}}\mathrm{i}^{r+\frac{1}{2}}}{z_n^{4r+1}(3+x/z_n^2)^{3r+\frac{1}{2}}} \sum_{t=0}^{r} \frac{(-\frac{1}{8})^t(3+x/z_n^2)^t(3r-t-\frac{1}{2})!}{(2r-2t)!\,t!}. \tag{41}$$

These coefficients can be expressed in closed form in terms of Legendre or Gegenbauer polynomials (Abramowitz & Stegun 1972), as follows:

$$\begin{aligned} T_r^{(n)} &= \frac{\sqrt{(2\pi)}\,\mathrm{i}^{r+\frac{1}{2}}}{2^r z_n^{4r+1}(3+x/z_n^2)^{(5r+1)/2}} \left[\frac{\mathrm{d}^r}{\mathrm{d}\zeta^r} \mathrm{P}_{3r}(\zeta)\right]_{\zeta=\{(3+x/z_n^2)/2\}^{-\frac{1}{2}}} \\ &= \frac{-\sqrt{2}\,\mathrm{i}^{r+\frac{1}{2}}(r-\frac{1}{2})!}{z_n^{4r+1}(3+x/z_n^2)^{2r+\frac{1}{2}}} \mathrm{C}_{2r}^{r+\frac{1}{2}}(\{(3+x/z_n^2)/2\}^{-\frac{1}{2}}). \end{aligned} \tag{42}$$

On the basis of the leading-order late terms formula (21) and the singulants (40) we expect the least terms of the sequences $T_r^{(1)}$, $T_r^{(2)}$, $T_r^{(3)}$ to be near $r = 10$, 10 and 15 respectively. Figure 10 shows that this is the case. If saddles 1 and 3 had been adjacent, the smallest $T_r^{(1)}$ and $T_r^{(3)}$ would have been near $r = 7$; the fact that they are not confirms that the nearest saddle, which dominates the asymptotics, is determined not simply by proximity (smallest $|F|$): adjacency is necessary too.

We also require the hyperterminant integrals, defined by (26) and (27), for the multiple scattering paths of figure 9. In the present case, where $k = 1$ and both paths starting from saddle 2 scatter back to 2, the first and second hyperterminants are

$$\begin{aligned} K_r^{(01)} &= \frac{(-1)^{\gamma_{01}}}{2\pi\mathrm{i}F_{01}^{N_0-r}} \int_0^\infty \mathrm{d}v \frac{v^{N_0-r-1}\exp(-v)}{1-v/F_{01}}, \\ K_r^{(012)} &= \frac{(-1)^{\gamma_{01}+\gamma_{12}}(-1)^{N_1-r-1}}{4\pi^2 F_{01}^{N_0-r}} \\ &\quad \times \int_0^\infty \mathrm{d}v_0 \frac{v_0^{N_0-N_1-1}\exp(-v_0)}{1-v_0/F_{01}} \int_0^\infty \mathrm{d}v_1 \frac{v_1^{N_1-r-1}\exp(-v_1)}{1+v_1/v_0}. \end{aligned} \tag{43}$$

(Note that here the subscripts 0, 1, 2 refer to orders of scattering, as in (24)–(28), and are not labels of saddles.) These integrals were computed as explained in Appendix B of I. We also needed the hyperterminants $K_r^{(0123)}$, which were approximated by replacing the $v$s in all the denominators by the stationary values of the other factors of the integrands, thereby uncoupling the integrals, which become proportional to factorials.

To the nearest integer, the rules (30) give the optimal truncation limits for the different paths of figure 9 (labelled by their saddle sequences) as

$$\left.\begin{aligned} N(2) = 10, \quad N(21) = N(23) = 5, \quad N(212) = N(232) = 2, \\ N(2121) = N(2123) = N(2321) = N(2323) = 1. \end{aligned}\right\} \tag{44}$$

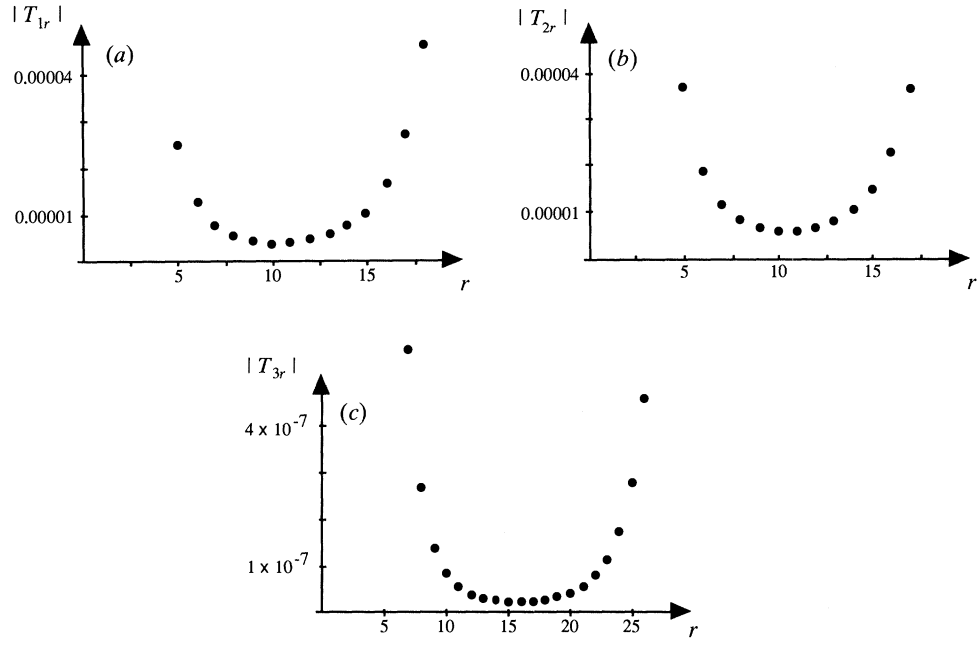


Figure 10. Magnitudes of asymptotic coefficients (41) for the three saddles in Pearcey's integral (35)–(37). Note the different scales for saddle 3.

Figure 11 shows the magnitudes of all the terms on all the scattering paths. This shows that the path with the largest remainder when hyperasymptotics terminates is 2121. As explained at the end of §4, this path controls the accuracy, and we should discard smaller terms from other scattering paths; these are the four terms below the line in figure 11.

Now we can evaluate the contributions to the terms in the hyperseries (24) and compare the partial sums with the 'exact' value of the Pearcey integral; this was computed from the convergent double series in ascending powers of $x$ and $y$, taking about 3000 terms to ensure sufficient accuracy. Obviously it is sensible to add the terms, in the various hyperseries, in order of decreasing magnitude. Figure 12 shows the relative errors |approximate/exact − 1| thus achieved. As expected, the errors decrease uniformly until the term 2121 at the end of the accuracy-controlling path is included. After that, there is no improvement, even though the last four terms decrease by nearly two orders of magnitude – indeed the very next term (2123) increases the error.

Table 1 shows some numerical values and relative errors of computations of $\mathrm{P}(7, 1+\mathrm{i})$. In addition to the 'exact' value, we include the lowest-order saddle-point approximation (that is, the first term of (3)), superasymptotics (that is, (3) truncated at its least term), and the best hyperasymptotic approximation, which includes the path 2121 and all larger terms. The ultimate error agrees well with the theoretical estimates (32) and (33), which give $1.103 \times 10^{-12}$.

Although our main aim was analytical understanding rather than the development of computational algorithms, we remark that hyperasymptotics seems to be numerically efficient: computation of the optimal approximation was about three

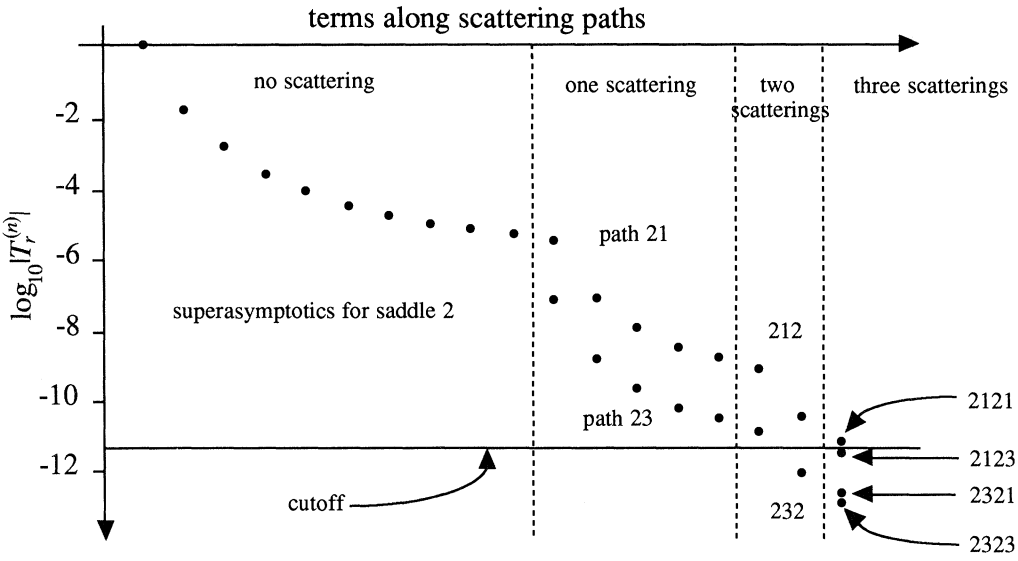


Figure 11. Magnitudes of the terms in the multiple scattering paths of figure 9 in the hyperasymptotics of Pearcey's integral.

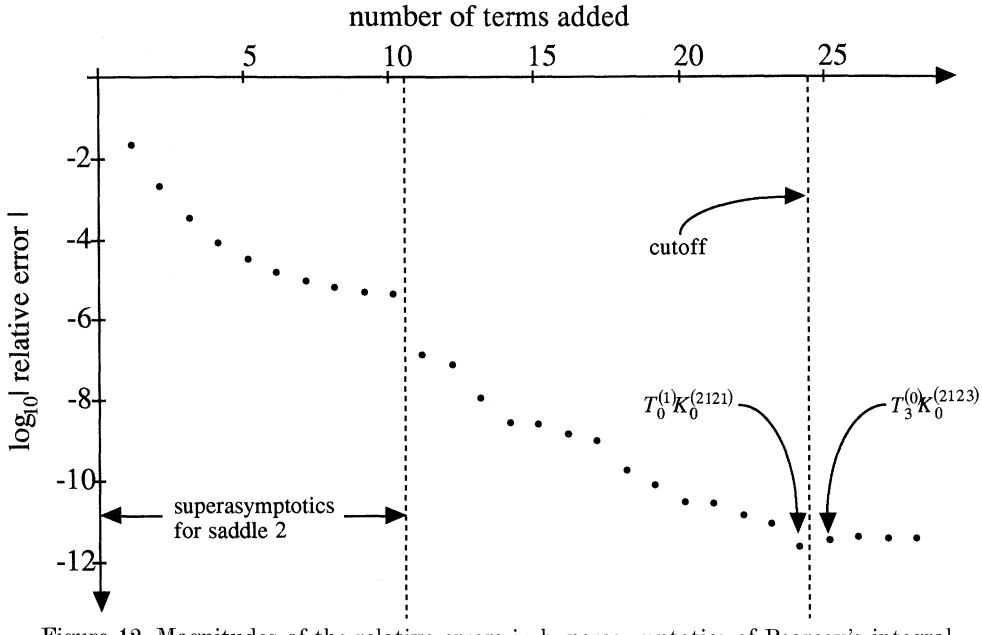


Figure 12. Magnitudes of the relative errors in hyperasymptotics of Pearcey's integral, incorporating successively smaller terms.

Table 1. *Approximations to the Pearcey integral (35)*

| level | approximation to P (7, 1+i) | \|approx./exact−1\| |
|---|---|---|
| lowest | 0.779703507027512+i0.765551648542315 | $1.496\times10^{-2}$ |
| super. | 0.788920520763900+i0.752101783262683 | $2.916\times10^{-6}$ |
| ultimate hyper. | 0.788922837595360+i0.752103959759701 | $1.535\times10^{-12}$ |
| exact | 0.788922837596969+i0.752103959759243 | 0 |

times faster than the 'exact' value. (The absolute time taken to calculate the 'exact' value, using the package Mathematica on an Apple Macintosh IIfx computer, was 400s.)

## 6. Concluding remarks

We have greatly extended the accuracy of the method of steepest descent, while retaining its numerical effectiveness as an integration technique, by basing it on the exact resurgence relation (19). The resulting iteration scheme (24)–(28) incorporates the effects of successively smaller exponentials, which arise from ever more distant groups of adjacent saddles and repeated scatterings from nearer ones. An attractive feature is the separation of non-universal properties characterizing the particular integral (1) being studied, and embodied in the raw asymptotic coefficients $T_r^{(n)}$, from the universal properties common to all integrals with saddles and embodied in the universal hyperterminant integrals (26)–(27). In a sense the history of asymptotics is repeating itself, albeit at a more refined stage, because as with Stokes's (1847) procedure of optimizing the raw asymptotic series by truncation at its least term, our iteration scheme too comes to a natural halt, representing an optimum level of approximation. We envisage several lines of further enquiry.

First, we hope mathematicians will be able to establish rigorous error bounds (rather than our estimates (32)–(33)). The explicit formula (28) for the hyperasymptotic remainder, which eliminates manipulations of divergent series, provides a natural starting-point for such investigations. It would be necessary to combine the errors for all the multiple scattering paths, which we have considered in isolation.

Second, there could be extensions to integrals (1) involving functions $f(z)$ and $g(z)$ with singularities. Clearly, each class of singularity would require special treatment.

Third, there is the question of 'beating the halting barrier', that is increasing the accuracy of the optimized scheme. Recall that for two saddles the error is roughly $\exp(-2.386|kF|)$. Further systematic improvement of the approximation ('ultra-asymptotics'?) would require evaluation of the roughly $\log_2|kF_{01*}|$-fold multiple-integral remainder (28). One possibility is to substitute the *convergent* series, in rising powers of the argument, for the function $T^{(s+1)}$. The motivation for this procedure is that the shortening of successive optimally truncated hyperseries can be regarded as a 'renormalization' of the original large parameter, which becomes effectively unity when the procedure halts. Preliminary indications are that fully halted hyperasymptotics can be terminated in this way, but that convergence is very slow.

Fourth, the $k$-dependence of hyperasymptotics should be unravelled. The first hyperseries (superasymptotics) is an exponential multiplied by a finite series in descending powers of $k$. The higher hyperseries have approximately this form, with smaller exponentials, but establishing the full $k$-dependence would involve approximating the hyperterminant integrals (26)–(27) to hyperasymptotic accuracy. The result could be that hyperasymptotics is a multiple-scale expansion whose large parameters are the different singulants.

Fifth, there is the extension to integrals with more than one variable. As well as being necessary to beat the halting barrier and approximate the hyperterminants, as just discussed, hyperasymptotics of multiple integrals would be useful in physics. Double integrals occur naturally in diffraction theory, where large $k$ corresponds to the geometrical-optics limit and small exponentials represent complex rays. Infinite-dimensional integrals occur in statistical mechanics and quantum field theory, where small exponentials represent instantons. It is tempting to regard hyperasymptotics

as a model for the feeble interaction of particles, represented by saddles. Each lowest saddle-point contribution gives the 'bare mass' of the corresponding particle; higher-order terms give the 'local renormalization' of this mass; the renormalization diverges, and hyperasymptotics describes the ultimate breakdown of locality, when the particles can no longer be considered in isolation.

Sixth, resurgence should be systematically applied to WKB theory for differential equations. In one dimension this would provide the extension of I to equations with effectively more than one transition point. The generalization of adjacency to transition points might justify the WKB topological rules of Knoll & Schaefer (1976), and complement the exact WKB analysis of Voros (1983). In more dimensions, one goal of resurgence would be to understand the semiclassical (small $\hbar$) expansions of quantum mechanics. For example, the expansion of the resolvent operator in powers of $\hbar$ (see Baltes & Hilf (1976) and Stewartson & Waechter (1971) for the case of quantum billiards, i.e. vibrating membranes) usually diverges, and we expect the divergence to contain information about the contributions from the periodic orbits of the corresponding classical system. These contributions are of order $\exp(\mathrm{i}S/\hbar)$, where $S$ is the action of the orbit. Each periodic-orbit contribution is itself the first term of a semiclassical expansion; it is likely that all these expansions diverge and that the divergences are interlocked by resurgence. For classically chaotic systems, the sum over all the periodic orbits itself diverges (for a discussion see Berry (1991)), and this divergence, like a similar one for the Riemann zeta function (Berry & Keating 1990), can also be interpreted by resurgence, albeit of a type different from that derived here.

We are grateful to Dr W. G. C. Boyd for carefully reading the manuscript and making many helpful suggestions. C.J.H. received financial support from SERC.

## Appendix A. The dangerous zeros

This concerns places where the quantity in braces in the denominator of (12) vanishes for real non-negative $u$, that is places where

$$\phi_n(z) \equiv k(f(z)-f_n) \tag{A 1}$$

is real and non-negative. We must show that there are no such 'dangerous zeros' in the region $\mathscr{R}$ defined as that swept by the deformation (by expansion) of the contour $\Gamma_n(\theta_k)$ (figure 2) described in §3. This is the region enclosed by the contours $C_m(-\sigma_{nm})$ through the saddles $m$ adjacent to $n$ (figure 3), together with the arcs at infinity joining their ends, and excluding the contour $C_n(\theta_k)$ itself (where $\phi_n(z)$ is real and non-negative by definition).

Consider the lines of constant phase of $\phi_n(z)$ issuing from the double zero of $\phi_n(z)$ at the saddle $z_n$; $z_n$ is a singularity of these lines, around which the phase changes by $4\pi$ (i.e. a phase dislocation of strength 2 (see Nye & Berry 1974)). Only on two of these lines, those where the phase of $\phi_n(z)$ is 0 and $2\pi$, is $\phi_n(z)$ real and non-negative, and these lines are the two halves of $C_n(\theta_k)$. The remaining phase lines fill a region bounded by the special phase lines (defined in the paragraph after (12)) through the adjacent saddles. This is precisely the region $\mathscr{R}$ which therefore cannot contain dangerous zeros.

The function $\phi_n(z)$ has zeros other than the double one at $z_n$. These are situated outside $\mathscr{R}$ and can be reached successively by starting from $z$ and passing over the

saddles $m \neq n$ along lines of constant phase of $\phi_n(z)$. Typically these other zeros are simple (i.e. phase dislocations of strength 1), with a dangerous zero (for given $u$) on one line of constant phase of $\phi_n(z)$ issuing from each of them. If $f(z)$ is an $M$th order polynomial, there are $M-2$ such simple zeros of $\phi_n(z)$, and hence $M-2$ dangerous zeros outside $\mathscr{R}$. Figure 8 shows an example with $M = 4$, where there are three saddles each with its associated function $\phi_n(z)$ which has two simple zeros.

## References


Abramowitz, M. & Stegun, I. A. 1972 *Handbook of mathematical functions.* Washington, D.C.: National Bureau of Standards.

Balian, R., Parisi, G. & Voros, A. 1979 In *Feynman path integrals* (ed. S. Albeverio *et al.*), pp. 337–360. *Lecture notes in physics*, vol. 106. Springer.

Baltes, H. P. & Hilf, E. R. 1976 *Spectra of finite systems.* Mannheim: B.-I. Wissenschaftsverlag.

Berry, M. V. 1989*a* *Proc. R. Soc. Lond.* A **422**, 7–21.

Berry, M. V. 1989*b* *Publ. Math. IHÉS* **68**, 211–221.

Berry, M. V. 1991 Some quantum-to-classical asymptotics. In *Chaos and quantum physics.* Les Houches Lecture Series 52 (ed. M. J. Giannoni & A. Voros). Amsterdam: North-Holland. (In the press.)

Berry, M. V. & Howls, C. J. 1990 *Proc. R. Soc. Lond.* A **430**, 653–668. (I of the text.)

Berry, M. V. & Keating, J. P. 1990 *J. Phys.* A **23**, 4839–4849.

Boyd, W. G. C. 1990 *Proc. R. Soc. Lond.* A **429**, 227–246.

Boyd, W. G. C. 1991 (In preparation.)

De Bruijn, N. J. 1958 *Asymptotic methods in analysis.* Amsterdam: North-Holland.

Dingle, R. B. 1973 *Asymptotic expansions: their derivation and interpretation.* New York and London: Academic Press.

Écalle, J. 1981 Les fonctions résurgentes (3 vols). Publ. Math. Université de Paris-Sud.

Écalle, J. 1984 Cinq applications des fonctions résurgentes. Preprint 84T62, Orsay.

Knoll, J. & Schaefer, R. 1976 *Ann. Phys., New York* **97**, 307–366.

Nye, J. F. & Berry, M. V. 1974 *Proc. R. Soc. Lond.* A **336**, 165–190.

Pearcey, T. 1946 *Phil. Mag.* **37**, 311–317.

Rakovic, M. J. & Solov'ev, E. A. 1989 *Phys. Rev.* A **40**, 6692–6694.

Stewartson, K. & Waechter, R. T. 1971 *Proc. Camb. phil. Soc.* **69**, 353–363.

Stokes, G. G. 1847 *Trans. Camb. phil. Soc.* **9**, 379–407. (Reprinted in *Mathematical and physical papers by the late Sir George Gabriel Stokes* (Cambridge University Press 1904), vol. II, pp. 329–357.)

Stokes, G. G. 1864 *Trans. Camb. phil. Soc.* **10**, 106–128. (Reprinted in *Mathematical and physical papers by the late Sir George Gabriel Stokes* (Cambridge University Press 1904), vol. IV, pp. 77–109.)

Voros, A. 1983 *Ann. Inst. H. Poincaré* **39**, 211–338.


*Received 1 March 1991; accepted 17 April 1991*